Crystal Structure of GABA-Aminotransferase, a Target for Antiepileptic Drug Therapy†

Paola Storici,*,‡,§ Guido Capitani,‡,§,|| Daniela De Biase,⊥ Markus Moser,§ Robert A. John,# Johan N. Jansonius,§ and Tilman Schirmer*,§

Division of Structural Biology, Biozentrum, University of Basel, Klingelbergstrasse 70, CH-4056 Basel, Switzerland, Dipartimento di Scienze Biochimiche, "A. Rossi Fanelli" Università La Sapienza, P.le Aldo Moro 5, I-00185 Rome, Italy, and School of Biosciences, University of Wales, Cardiff CF1 3US, United Kingdom

Received March 1, 1999; Revised Manuscript Received April 28, 1999

ABSTRACT: γ-Aminobutyrate aminotransferase (GABA-AT), a pyridoxal phosphate-dependent enzyme, is responsible for the degradation of the inhibitory neurotransmitter GABA and is a target for antiepileptic drugs because its selective inhibition raises GABA concentrations in brain. The X-ray structure of pig GABA-AT has been determined to 3.0 Å resolution by molecular replacement with the distantly related enzyme ornithine aminotransferase. Both ω-aminotransferases have the same fold, but exhibit side chain replacements in the closely packed binding site that explain their respective specificities. The aldimines of GABA and the antiepileptic drug vinyl-GABA have been modeled into the active site.

GABA-AT[1] is a target for neuroactive drugs because its inhibition alters the balance between its substrate GABA and the product L-glutamate (*1*), which are respectively the major inhibitory and excitatory neurotransmitters in brain. Selective inactivation by vinyl-GABA, a mechanism-based inhibitor of the enzyme (*2*), is already successfully applied in treatment of epilepsy (*3*). Several other serious neurological disorders, including Huntington's disease, schizophrenia, and Alzheimer's disease, are also associated with abnormally low levels of GABA and might also be expected to respond to inhibition of the enzyme by appropriate compounds (*4*).

GABA-AT belongs to a large family of homologous aminotransferases (*5*) which operate by the same basic mechanism consisting of two coupled half-reactions in which the PLP-cofactor oscillates between its pyridoxal and pyridoxamine forms. Most of these enzymes, including GABA-AT and ornithine aminotransferase (OAT), use 2-oxoglutarate and L-glutamate in the return half-reaction, whereas the forward reaction differs according to the specificity of each enzyme (*6*). In GABA-AT, the specific reaction converts GABA to succinic semialdehyde (*7*). Scheme 1 shows the two half-transamination reactions catalyzed by GABA-AT.

Scheme 1

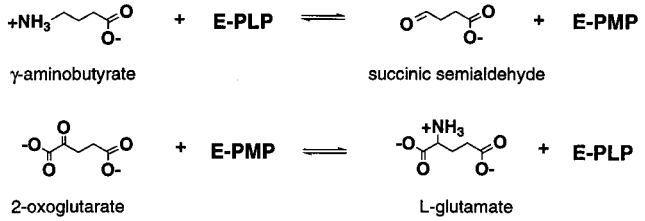

Understanding the structural basis of substrate specificity is important for the development of inhibitors. This is especially true when closely similar substrates are recognized by homologous enzymes, such as GABA and ornithine by the ω-aminotransferases GABA-AT and OAT, respectively. Here, we report the crystal structure of pig liver GABA-AT, which is 96% identical to the human brain enzyme (*8*). We expect that the availability of the GABA-AT structure will assist the rational design of new neuroactive compounds of value in the treatment of the several neurological and psychiatric disorders accompanied by altered GABA levels.

MATERIALS AND METHODS

Crystallization and Data Collection. The protein was purified from pig liver in the presence of 1 mM EDTA following the procedure described in (*9*). Crystallization was performed as previously described (*10*) in the presence of 40 mM sodium acetate (pH 5.6) and 1 mM PLP, without reducing agents. Data were collected from a single crystal on an Enraf-Nonius FAST area detector diffractometer at room temperature. Data processing and reduction (Table 1) were performed with MADNES (*11*) and programs from the CCP4 suite (*12*).

Structure Solution. The GABA-AT structure was solved by molecular replacement employing the program AMORE (*13*). Taking into account that the sequences of both OAT

† This work was in part supported by Swiss National Science Foundation Grant 31-36432.92 to J.N.J. and by italian grants from MURST and CNR, Target Project on Biotechnology.

* To whom correspondence should be addressed. (T.S.) Phone: +41-61-2672089. Fax: +41-61-2672109. Email: schirmer@ubaclu.unibas.ch. (P.S.) Phone: +41-61-2672092. Email: storici@ubaclu.unibas.ch.

‡ These authors have contributed equally to this work.

§ University of Basel.

|| Current address: Institute of Biochemistry, University of Zürich, Winterthurerstrasse 190, CH-8057 Zürich, Switzerland.

⊥ "A. Rossi Fanelli" Universita La Sapienza.

University of Wales.

[1] Abbreviations: DGD, dialkylglycine decarboxylase; GABA, γ-aminobutyric acid; GABA-AT, γ-aminobutyrate aminotransferase; OAT, ornithine aminotransferase; PLP, pyridoxal 5′-phosphate; PMP, pyridoxamine 5′-phosphate; rms, root-mean-square; *, denotes residues from the second subunit in the dimer.

10.1021/bi990478j CCC: $18.00
Published on Web 06/09/1999

Table 1: Data Collection and Refinement Statistics

unit cell dimensions[a]	$a = 69.9$ Å, $b = 230.4$ Å, $c = 72.8$ Å, $\beta = 109.4°$
space group	$P2_1$
number of monomers per asymmetric unit	4
resolution range (Å)	28−3.0
number of reflections	39236
R_{sym} (%)[b]	13.0
$\langle I\rangle/\sigma(I)$	5.1
completeness (%)	90.8
multiplicity	2.2
R_{factor} (%)[c]	18.6
R_{free} (%)[d]	21.7
number of protein atoms (non-H)	3678
number of cofactor atoms	15
number of acetate atoms	4
number of water molecules	13
mean overall *B*-factor (Å^2)	26.1
rms deviation bond lengths (Å)[e]	0.013
rms deviation bond angles (deg)[e]	1.68
Ramachandran plot statistics[f]	
residues in most favored regions (%)	84.1
residues in disallowed regions	Lys329, Met332

[a] The unit cell is virtually identical to that reported previously (*10*), but an alternative unit cell assignment was used. [b] $R_{sym} = \sum_{hkl}\sum_i(|I(hkl) - \langle I(hkl)\rangle|)/\sum_{hkl}\sum_i\langle I(hkl)\rangle$. [c] R_{factor} is the conventional R factor. [d] R_{free} is the R factor calculated with 4% of the data that were not used for refinement. [e] rms deviation from ideal stereochemistry. [f] Calculated with program PROCHECK (*18*).

(*14*) and dialkylglycine decarboxylase (DGD) (*15*) show similar levels of sequence identity to GABA-AT, these two dimeric structures (PDB codes: 1OAT and 2DKB) were superimposed. Those parts of the dimeric OAT that aligned well with the DGD structure were used as the search model for molecular replacement, thus comprising 66% of the GABA-AT main chain. Subsequently, all side chains were pruned to serine. The cross-rotation function did not reveal outstanding peaks. Furthermore, the translation functions computed for the top 50 orientations did not yield a clear signal. Each of these potential solutions for the first dimer of the asymmetric unit was fixed, and 49 translation functions were calculated for the second dimer, one for each orientation suggested by the cross-rotation list. After rigid-body refinement, the best solution showed reasonable packing and was used to calculate an initial set of phases. It had a relatively poor correlation coefficient of 0.14 ($R = 54.2\%$), which was only slightly above the value of the second best (0.12). A self-rotation map computed from the structure factors of the top-rating solution approximated well the experimental self-rotation map. Density modification (including averaging over the four GABA-AT subunits) and phase extension from 4.4 to 3.0 Å were performed with DM (*12*) using a mask derived from the full OAT model. The resulting map was interpretable and clearly showed the cofactor, which was not part of the search model.

Phase Improvement and Model Refinement. To improve the input map for the phase extension procedure, the search model was complemented by introducing the GABA-AT sequence and pre-refined at 3 Å, using program X-PLOR (*16*) with strict NCS and tight geometric and thermal restraints. This model was combined with a skeletonized representation [generated by the program MAPMAN (*17*) and weighted by a factor of 0.3−0.4] of that part of the DM density that was not accounted for by the partial GABA-AT model. The phase set derived from this combined model was used for another round of phase extension and density modification. The procedure was repeated after manual correction and extension of the model. Finally, the model was refined with strict NCS constraints using simulated annealing torsion angle refinement followed by strongly restrained individual *B*-factor refinement (program X-PLOR). The acetate ligand was included only in the last round. The stereochemistry of the model was validated with PROCHECK (*18*). The final refinement statistics are given in Table 1.

Model Building. The models of GABA and *S*-vinyl-GABA external aldimines in complex with GABA-AT were energy minimized with X-PLOR. The protein atoms were restrained by harmonic potentials (20 kcal mol^{-1} Å^2 for Cα atoms, 3 kcal mol^{-1} Å^2 for all others).

Coordinates. The coordinates for GABA-AT have been deposited in the Brookhaven Protein Data Bank (accession code 1GTX).

RESULTS AND DISCUSSION

Structure Solution and General Fold. The crystal structure of GABA-AT was solved by molecular replacement using the model of OAT (*14*) with which it shares 17.4% sequence identity. Due to the low structural similarity and the presence of two dimers per asymmetric unit, the cross-rotation function was not readily interpretable. The problem was solved by systematic translation function calculations to test all possible combinations of orientations as given by the 50 highest peaks in the cross-rotation function. Subsequent 4-fold molecular averaging and phase extension to 3 Å yielded well-defined unbiased electron density, which was continuous for the entire polypeptide chain except for the first 10 residues at the N-terminus.

The success of this approach is remarkable, since the dimeric search model comprised only 24% of the atoms of the two dimers contained in the asymmetric unit. Superposition of the final GABA-AT monomer model with OAT shows a relatively large rms deviation of 2.1 Å for 390 Cα positions. This demonstrates that, if it is used exhaustively, the molecular replacement method is more powerful than has hitherto been believed.

The mature enzyme is an α_2-dimer with 472 residues per subunit. The two monomers are tightly intertwined, and the two PLP cofactors are located close to the subunit interface (Figure 1a). About a quarter of the monomer surface is buried upon dimer formation. Structural domains are not easily recognized because of the compactness of the molecule. The following domain classification is based on assignments made with the prototype of the family, aspartate aminotransferase (*6, 19*), with which it shares the same basic fold.

The large domain (residues 81−375), which forms most of the subunit interface, comprises a central 7-stranded β-sheet surrounded by 10 α-helices. The N-terminal domain (residues 11−71) is composed of one α-helix, which contacts the large domain of the other subunit, and a four-stranded antiparallel β-sheet, which forms one of the active site walls. The C-terminal domain (residues 376−472) is found at the periphery of the dimer and is comprised of a four-stranded antiparallel β-sheet covered on one side by three helices.

The GABA-AT fold is most closely similar to that of OAT (*14*) and DGD (*15*), and, to a lesser extent, to that of

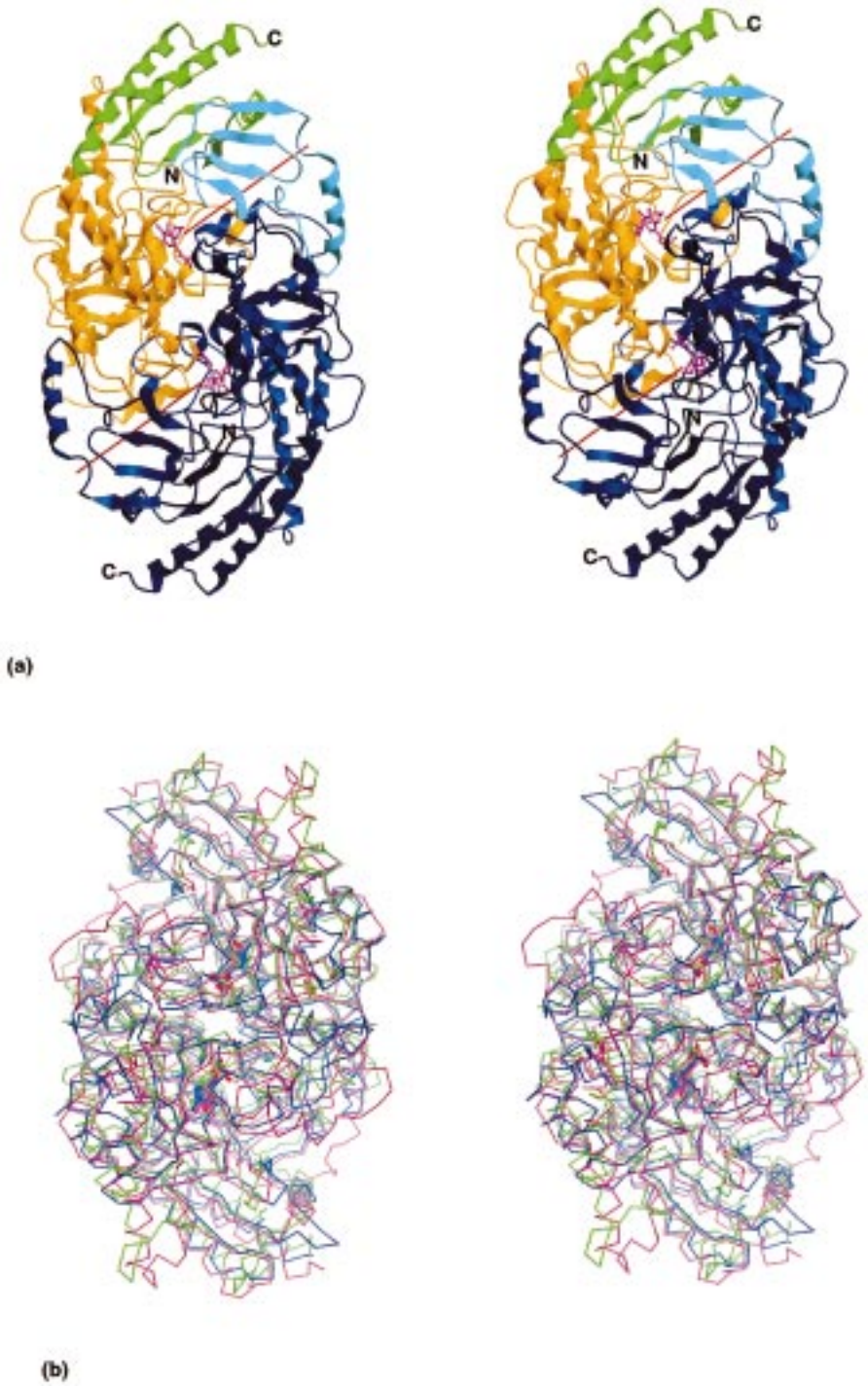

FIGURE 1: General fold of GABA-AT dimer. (a) Cartoon model of the GABA-AT dimer viewed along the molecular 2-fold symmetry axis, with the PLP cofactors shown in ball-and-stick representation. The N-terminal domain is shown in cyan, the large domain in orange, and the C-terminal domain in green. The two red lines show the active site entries. (B) Superimposition of the Cα traces of GABA-AT (magenta), OAT (blue), and DGD (green). The view is from the opposite direction compared to the view in panel a. The rms deviations between the Cα positions of the GABA-AT monomer and those of OAT and DGD are 2.1 Å (390 equivalent Cα atoms) and 2.2 Å (388 equivalent Cα atoms), respectively. The figure has been prepared with program DINO (*30*).

glutamate semialdehyde aminomutase (*20*). A superposition of the Cα trace with that of OAT and DGD is given in Figure 1b. Compared to the other enzymes (Figure 2), GABA-AT shows after helix 5 a major insertion, which partly adopts a helical conformation (helix 6). Helix 9 is considerably extended and has an unusually high density of cationic residues at its C-terminus (five out of seven residues are lysines and one is an arginine). Together with their symmetry-related counterparts, these two motifs constitute an almost continuous patch comprising approximately 25% of the dimer surface. In DGD and OAT, the corresponding part of the surface is involved in dimer−dimer interactions to form a tetramer (*15*) and a hexamer (*14*), respectively. There is no indication that GABA-AT forms higher oligomers, but it is possible that this part of the surface is involved in interaction with other cellular components. The formation of a bi-enzyme complex with succinic semialdehyde dehydrogenase, the enzyme that catalyzes the next reaction in

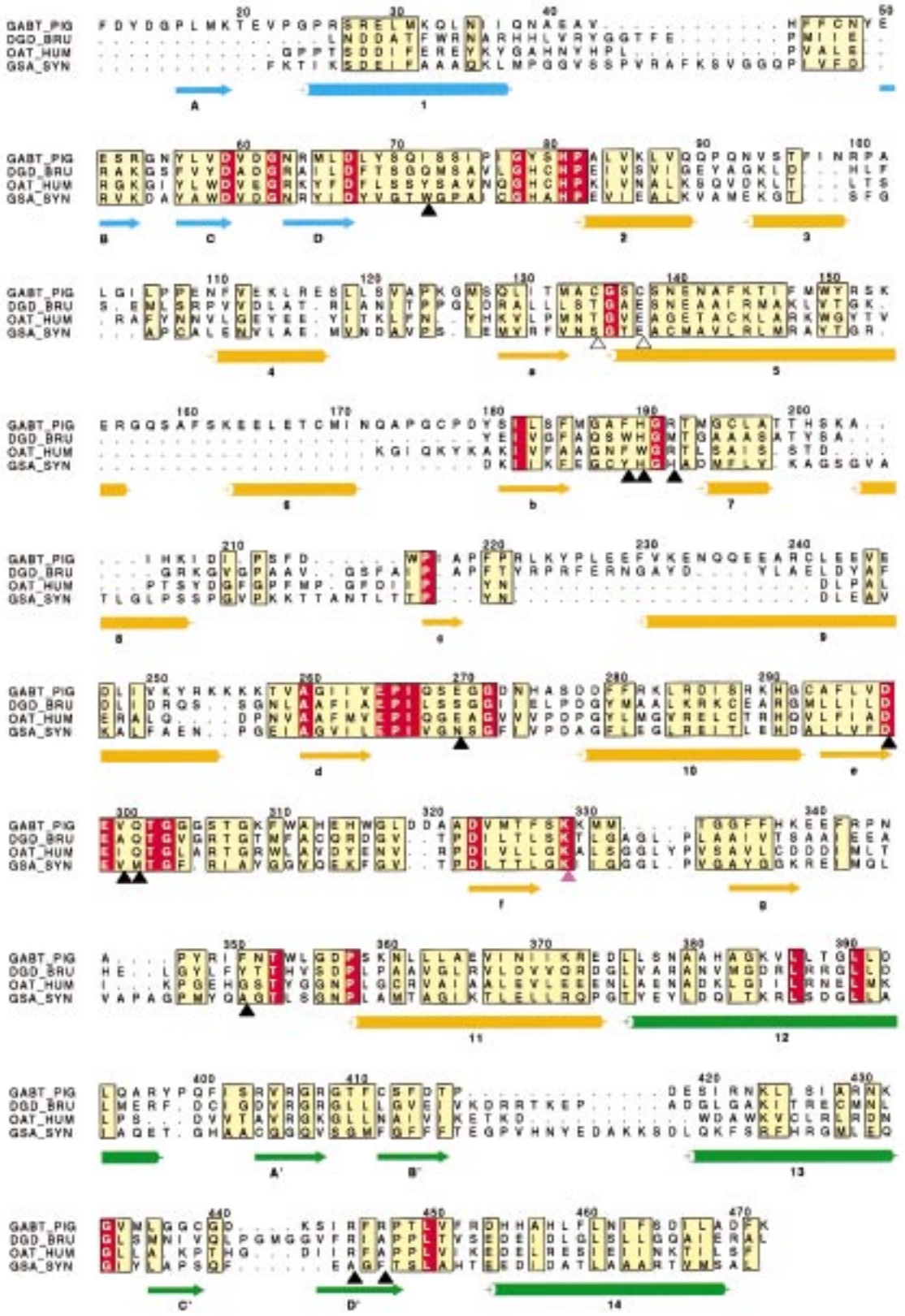

FIGURE 2: Structure-based sequence alignment using the DALI server (*31*) of pig GABA-AT with those members of subgroup II of the aminotransferase α-family that show closest structural similarity. Abbreviations used: GABT_PIG, 4-aminobutyrate aminotransferase of pig; DGD_BRU, dialkylglycine decarboxylase from *Pseudomonas cepacia*; OAT_HUM, human ornithine aminotransferase; GSA_SYN, glutamate-1-semialdehyde aminomutase from *Synechococcus sp.* Yellow boxes denote conserved residues, red boxes identical residues. Secondary structural elements of GABA-AT are shown, and are colored according to the domain subdivision shown in Figure 1a. Black arrows mark active site residues. A magenta arrow points to the lysine to which, in all four enzymes, the PLP cofactor is covalently bound. Cysteines 135 and 138 of GABA-AT, which form a disulfide bridge, are marked by white arrows. The numbering is based on the mature GABA-AT sequence as published by De Biase et al. (*32*).

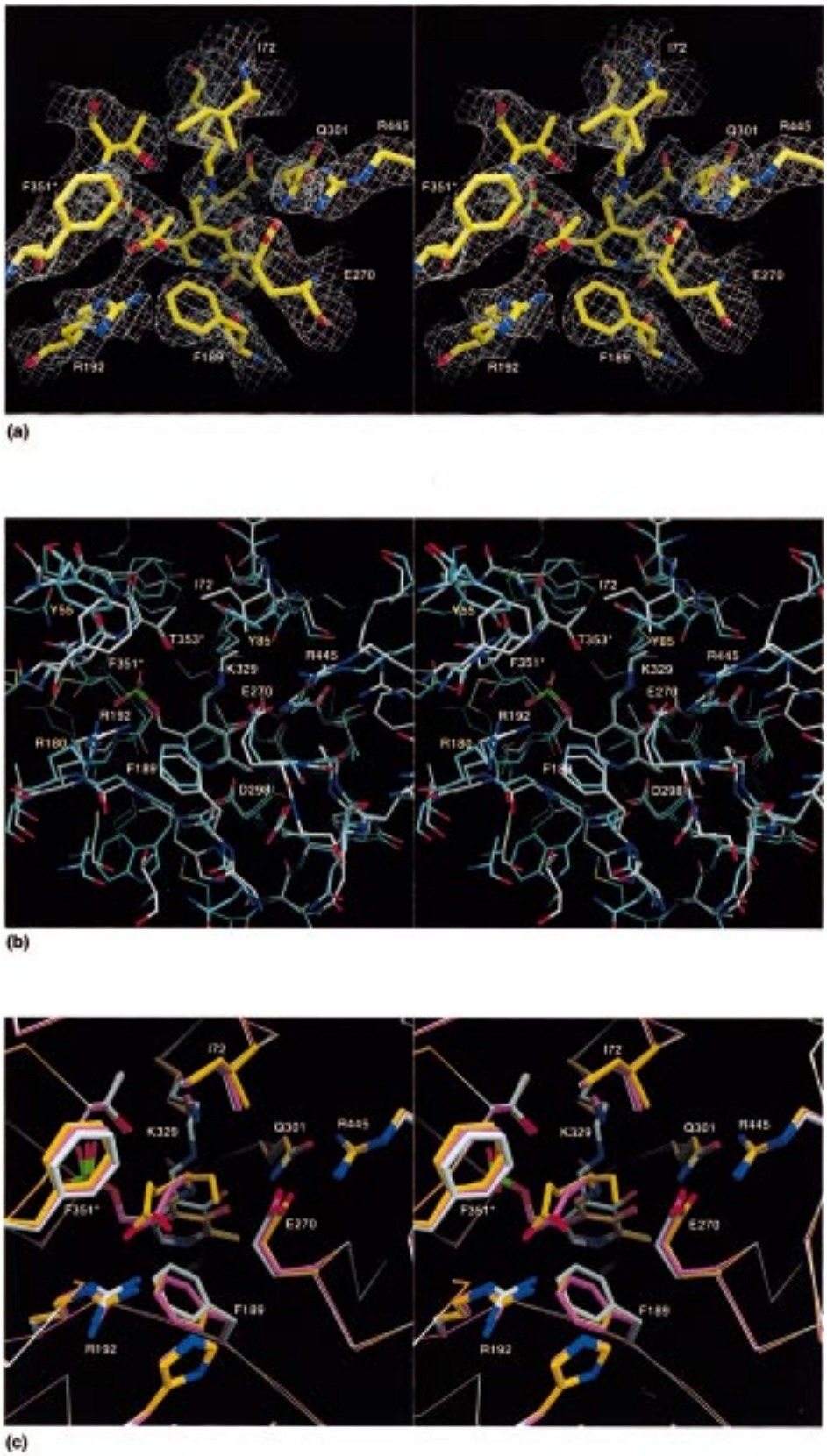

FIGURE 3: Stereo drawings (prepared with program DINO) (*30*) of the active site of GABA-AT. (A) Final model electron density map (contour level 1.2 σ) as derived from the averaging and phase extension procedures. The extra density close to Arg192 has been modeled as an acetate molecule. (b) Superimposition of the active sites of GABA-AT (white) and OAT (cyan), similar orientation as in panel a. Important residues of GABA-AT are labeled in white; a few corresponding residues of OAT are labeled in yellow. (c) Energy-minimized models of the external aldimine of the natural substrate GABA (magenta) and of the inhibitor vinyl-GABA (orange) superimposed on the native structure (white). Only relevant protein side chains are shown.

the metabolic sequence, has been reported (*21*).

A unique feature of GABA-AT is a cluster of cysteines at the dimer interface. This is formed by cysteines 135 and 138 (at the N-terminus of helix 5, close to the PLP phosphate group) together with their symmetry mates from the other subunit. The electron density indicates the presence of two intrachain disulfides, although additional density is found between them on the symmetry axis. Formation of an interchain disulfide link appears not to be possible without changes in the course of the main chain. Also, the presence of a bridging metal ion would be incompatible with the predominant cysteine conformation. Thus, the residual density may indicate partially oxidized cysteines, since no reducing agent was present during crystallization.

Active Site. The PLP cofactor is deeply buried within the protein matrix and is involved in many specific interactions (Figure 3) which have counterparts in all other PLP enzymes, which share this fold (*22*). The 4′-aldehyde is covalently connected to the ϵ-amino group of Lys329 via a Schiff base linkage. The phosphate group of the cofactor interacts with the N-terminus of helix 5 and is further held in place by five H-bonds donated by Gly136, Ser137, and Thr353* (the asterisk denotes a residue from the second subunit). The pyridine ring is sandwiched between Phe189 and Val300, and its nitrogen forms a salt bridge with Asp298. As inferred by sequence comparison, all active site residues within a distance of 10 Å from the cofactor have identical counterparts in the human brain GABA-AT.

Figure 3b shows the close resemblance between the substrate binding pockets of GABA-AT and OAT. Arg192, like Arg180 of OAT, which interacts with the carboxylate group of ornithine analogues (*23*, *24*), is correctly positioned and accessible for binding the carboxylate of GABA. The presence of extra electron density in the active site, interpreted as an acetate molecule forming a double hydrogen-bonded ion pair with Arg192, confirms the binding role of this residue (Figure 3a). Acetate, which was present in the crystallization setup, is known to be a competitive inhibitor of GABA-AT (*25*).

Arg445 is fully conserved in the α-family of aminotransferases (*5*). Whereas in aspartate aminotransferase it is free and known to bind the substrates' α-carboxylates (*26*), in GABA-AT, this arginine is shielded by a salt bridge with Glu270, a situation that has hitherto been observed only for OAT (Figure 3b). GABA-AT and OAT have similar specificity, in that each acts on the ω-amino group of monocarboxylic acids and on the α-amino group of dicarboxylic acids. It seems likely that the structural basis proposed for this dual specificity in OAT (*23*) applies also to GABA-AT. Thus, the single carboxylate of GABA and succinic semialdehyde would bind only to Arg192, whereas the dicarboxylic substrates would also require opening of the Glu270−Arg445 ion pair to expose a second basic anchor point. Similar conclusions have been previously drawn from a homology modeling study of GABA-AT (*27*).

Two major differences between the active sites of GABA-AT and OAT (Figure 3b) probably determine the different substrate specificities of these enzymes. In GABA-AT, Phe351* and Ile72 replace tyrosines 55 and 85 of OAT, respectively. Notably, the former substitution concerns nonhomologous residues that even belong to different subunits. The phenyl ring of residue 351* contributes to the narrowing of the active site (Figure 3b), and both replacements render it more hydrophobic. This probably reflects the requirements for binding of the substrate GABA, which, compared to ornithine, is shorter by one methylene group and lacks the α-amino group. It is known that the hydroxyl group of Tyr55 interacts with the α-amino group of ornithine in OAT (*23*).

Modeling of GABA and Vinyl-GABA Binding. Modeling of the GABA-PLP external aldimine intermediate into the active site of the enzyme (Figure 3c) was straightforward. Upon appropriate tilting of the cofactor ring, known to accompany external aldimine formation in PLP enzymes (*23*, *24*, *28*), the α-carboxylate of the GABA-PLP aldimine can easily reach Arg192 and form a bifurcated salt-bridge. This positions the *pro-S* proton of the Cγ carbon appropriately for abstraction by Lys329, in accordance with the known stereospecificity of the reaction (*29*). Alternative binding modes appear unlikely due to the constraints imposed by the narrow active site.

The *S*-isomer of vigabatrin (γ-vinyl-GABA), a widely used antiepileptic drug, irreversibly inhibits the enzyme (*2*). Figure 3c shows that the external aldimine of this compound can bind in a mode very similar to that of GABA, with the γ-proton again pointing toward the Lys329 so that it can be successfully abstracted. Furthermore, Lys329 would be at the correct distance from the vinyl group to activate the inhibitor as proposed (*9*). Future crystallographic studies of complexes of GABA-AT with different inhibitors or substrate analogues will show their precise binding mode and reveal any movements of active site residues occurring upon binding.

The present structure not only demonstrates the extraordinary power of molecular replacement in conjunction with density modification, but also provides an accurate basis for the development of new anticonvulsant drugs, in that all the active site residues are fully conserved in the human brain enzyme.

ACKNOWLEDGMENT

We thank R. Müller and U. Sauder for technical support in purification and crystallization.

REFERENCES

1. Schwartz, J. H. (1991) in *Principles of neural science* (Kandel, E. R., Schwartz, J. H., and Jessell, T. M., Eds.) pp 217−217, Prentice Hall International, Norwalk.
2. Lippert, B., Metcalf, B. W., Jung, M. J., and Casara, P. (1977) *Eur. J. Biochem. 74*, 441−445.
3. Davies, J. A. (1995) *Seizure 4*, 267−271.
4. Johnston, G. A. R., and Balcar, V. J. (1989) in *GABA enzymes and transport systems* (Bowery, N. G., and Nisticò, G., Eds.) pp 1−23, Pythagora Press, Rome−Milan.
5. Mehta, P. K., Hale, T. I., and Christen, P. (1993) *Eur. J. Biochem. 214*, 549−561.
6. Jansonius, J. N. (1998) *Curr. Opin. Struct. Biol. 8*, 759−769.
7. Cooper, A. J. (1985) *Methods Enzymol. 113*, 80−82.
8. De Biase, D., Barra, D., Simmaco, M., John, R. A., and Bossa, F. (1995) *Eur. J. Biochem. 227*, 476−480.
9. De Biase, D., Barra, D., Bossa, F., Pucci, P., and John, R. A. (1991) *J. Biol. Chem. 266*, 20056−20061.
10. Markovic-Housley, Z., Schirmer, T., Fol, B., Jansonius, J. N., DeBiase, D., and John, R. A. (1990) *J. Mol. Biol. 214*, 821−823.
11. Messerschmidt, A., and Pflugrath, J. W. (1987) *J. Appl. Crystallogr. 20*, 306−315.

12. Collaborative computational project number 4 (1994) *Acta Crystallogr. D50*, 760−763.
13. Navaza, J. (1994) *Acta Crystallogr. A50*, 157−163.
14. Shen, B. W., Hennig, M., Hohenester, E., Jansonius, J. N., and Schirmer, T. (1998) *J. Mol. Biol. 277*, 81−102.
15. Toney, M. D., Hohenester, E., Keller, J. W., and Jansonius, J. N. (1995) *J. Mol. Biol. 245*, 151−179.
16. Brünger, A. T. (1992) *X-PLOR manual, version 3.1*, Yale University, New Haven, CT.
17. Kleywegt, G. J., and Jones, T. A. (1996) *Acta Crystallogr. D52*, 826−828.
18. Laskowski, R. A., MacArthur, M. W., Moss, D. S., and Thornton, J. M. (1993) *J. Appl. Crystallogr. 26*, 283−291.
19. Ford, G. C., Eichele, G., and Jansonius, J. N. (1980) *Proc. Natl. Acad. Sci. U.S.A. 77*, 2559−2563.
20. Hennig, M., Grimm, B., Contestabile, R., John, R. A., and Jansonius, J. N. (1997) *Proc. Natl. Acad. Sci. U.S.A. 94*, 4866−4871.
21. Hearl, W. G., and Churchich, J. E. (1984) *J. Biol. Chem. 259*, 11459−11463.
22. John, R. A. (1995) *Biochim. Biophys. Acta 1248*, 81−96.
23. Storici, P., Capitani, G., Mueller, R., Schirmer, T., and Jansonius, J. N. (1999) *J. Mol. Biol. 285*, 297−309.
24. Shah, S. A., Shen, B. W., and Brünger, A. T. (1997) *Structure 5*, 1067−1075.
25. John, R. A., and Fowler, L. J. (1976) *Biochem. J. 155*, 645−651.
26. Malashkevich, V. N., Toney, M. D., and Jansonius, J. N. (1993) *Biochemistry 32*, 13451−13462.
27. Toney, M. D., Pascarella, S., and De Biase, D. (1995) *Protein Sci. 4*, 2366−2374.
28. Jansonius, J. N., and Vincent, M. G. (1987) in *Biological Macromolecules and Assemblies: Active sites of enzymes* (Jurnak, F. A., and McPherson, A., Eds.) Vol. 3, pp 187−285, J. Wiley and Sons, New York.
29. Bouclier, M., Jung, M. J., and Lippert, B. (1979) *Eur. J. Biochem. 98*, 363−368.
30. Philippsen, A. (1998) http://www.bioz.unibas.ch/∼xray/dino.
31. Holm, L., and Sander, C. (1993) *J. Mol. Biol. 233*, 123−138.
32. De Biase, D., Maras, B., Bossa, F., Barra, D., and John, R. A. (1992) *Eur. J. Biochem. 208*, 351−357.

BI990478J